

Proton Radiation Damage Experiment on P-Channel CCD for an X-ray CCD camera onboard the Astro-H satellite

Koji Mori^a, Yusuke Nishioka^{a,b}, Satoshi Ohura^a, Yoshiaki Koura^a, Makoto
Yamauchi^a, Hiroshi Nakajima^c, Shutaro Ueda^c, Hiroaki Kan^c, Naohisa
Anabuki^c, Ryo Nagino^c, Kiyoshi Hayashida^c, Hiroshi Tsunemi^c, Takayoshi
Kohmura^d, Shoma Ikeda^d, Hiroshi Murakami^e, Masanobu Ozaki^f, Tadayasu
Dotani^f, Yukie Maeda^g, Kenshi Sagara^h

^a*Department of Applied Physics and Electronic Engineering, Faculty of Engineering,
University of Miyazaki, 1-1 Gakuen Kibanadai-Nishi, Miyazaki, 889-2192, Japan*

^b*Technical center, Faculty of Engineering, University of Miyazaki, 1-1 Gakuen
Kibanadai-Nishi, Miyazaki, 889-2192, Japan*

^c*Department of Earth and Space Science, Graduate School of Science, Osaka University,
1-1 Machikaneyama, Toyonaka, Osaka, 560-0043, Japan*

^d*Physics Department, Kogakuin University, 2665-1, Nakano, Hachioji, 192-0015, Japan*

^e*Department of Physics, Faculty of Science, Rikkyo University, 3-34-1, Nishi-Ikebukuro,
Toshima-ku, Tokyo, 171-8501, Japan*

^f*Institute of Space and Astronautical Science, Japan Aerospace Exploration Agency,
3-1-1 Yoshinodai, Chuo-ku, Sagamihara, Kanagawa 252-5210, Japan*

^g*Faculty of Engineering, University of Miyazaki, 1-1 Gakuen Kibanadai-Nishi, Miyazaki,
889-2192, Japan*

^h*Department of Physics, Kyushu University, 6-10-1 Hakozaki, Higashi-ku, Fukuoka
812-8581, Japan*

Abstract

We report on a proton radiation damage experiment on P-channel CCD newly developed for an X-ray CCD camera onboard the Astro-H satellite. The device was exposed up to 10^9 protons cm^{-2} at 6.7 MeV. The charge transfer inefficiency (CTI) was measured as a function of radiation dose. In comparison with the CTI currently measured in the CCD camera onboard the Suzaku satellite for 6 years, we confirmed that the new type of P-channel

CCD is radiation tolerant enough for space use. We also confirmed that a charge-injection technique and lowering the operating temperature efficiently work to reduce the CTI for our device. A comparison with other P-channel CCD experiments is also discussed.

25 *Keywords:* P-channel CCD, Proton radiation damage, Charge-injection

26 **1. Introduction**

27 Charge-coupled devices (CCDs) have an almost 20-years long history as
28 space-borne detectors for X-ray astronomy. The ASCA satellite for the first
29 time employed X-ray photon counting CCDs[1], which were front-illuminated
30 (FI) devices with a depletion layer thickness of about 30 μm . Subsequent
31 Japanese X-ray satellite Suzaku carries, in addition to FI CCDs, a back-
32 illuminated (BI) CCD that significantly improved the detection efficiency for
33 soft X-ray photons down to 0.3 keV[2]. However, the depletion layer thickness
34 of the BI CCD was still limited to about 40 μm . The X-ray CCDs flown to
35 space so far were all made from P-type silicon wafers, namely N-channel
36 CCDs. Recently, a new type of P-channel CCD has become available with a
37 thick depletion layer of a few hundred μm [3]. We employ the new P-channel
38 CCD for Soft X-ray Imager (SXI)[4, 5], a new CCD camera onboard the
39 upcoming Astro-H satellite[6]. Using the P-channel CCD as a BI device with
40 a depletion layer thickness of 200 μm , high detection efficiency for both hard
41 and soft X-ray photons can be achieved.

42 Since P-channel CCDs have no performance experience in space, their
43 radiation hardness is an issue to be examined before launch. The primary
44 source of radiation damage of CCD is cosmic-ray protons, which produce

45 displacement damage in silicon resulting in the formation of carrier traps.
 46 Traps in the channel region capture charge carriers during transfer. Then,
 47 the charge transfer inefficiency (CTI), a fraction of charge loss per one pixel
 48 transfer, is frequently used as a measure of radiation damage for X-ray CCDs.
 49 There are several experimental reports indicating that P-channel CCDs are
 50 actually radiation harder than conventional N-channel CCDs in terms of
 51 the CTI[7, 8, 9]. The greater radiation hardness of P-channel CCDs may
 52 be explained by the difference of carrier traps in the two different type of
 53 CCDs[10, 7]. Proton-induced formation of divacancy hole traps is considered
 54 to be less favorable in a P-channel CCD compared to that of phosphorus-
 55 vacancy electron traps in an N-channel CCD[8]. However, it is also suggested
 56 that other kind of traps are possibly produced and they may adversely in-
 57 crease the CTI in a P-channel CCD[11].

58 In relation to the radiation hardness of the device, mitigating the radi-
 59 ation damage effect is also important. A charge-injection (CI) technique is
 60 one of such mitigation methods[12, 13, 14]. In this technique, charges are
 61 intentionally injected to selected rows which are regularly spaced. Then,
 62 the injected charges work as sacrifices to fill traps and following real X-ray-
 63 induced charges are transferred with lesser charge loss. The CI has been
 64 verified to effectively reduce the CTI in the case of the Suzaku CCDs[12].
 65 Lowering operating temperature of CCDs also reduced the CTI in the case
 66 of the Chandra and XMM-Newton CCDs[15, 16].

67 In this paper, we report on a proton radiation damage experiment on
 68 our newly developed P-channel CCD. We here describe how radiation-hard
 69 our new device is and how our mitigation methods work once the device is

70 damaged.

71 **2. Experiment**

72 *2.1. P-channel CCD used in this experiment*

73 We developed a P-channel BI CCD for the SXI, Pch-NeXT4, in collabo-
74 ration with Hamamatsu Photonics K.K.[4, 5] (“NeXT” is the former project
75 name of the Astro-H satellite). The Pch-NeXT4 is a frame transfer type
76 CCD with an imaging area of 30.72 mm square. There are 1280×1280 phys-
77 ical pixels in the imaging area, which will be 640×640 logical pixels after
78 on-chip 2×2 binning. There are four readout nodes, and we nominally use
79 two of them.

80 There were two CCDs used in this experiment. One was the same type
81 of CCD as Pch-NeXT4, and the other was a smaller size CCD but made in
82 the same manufacturing process as that of Pch-NeXT4. We hereafter refer
83 to the former and the latter as large-CCD and mini-CCD, respectively.

84 *2.2. Experimental setup*

85 We performed our proton radiation damage experiment at the Kyushu
86 University tandem accelerator laboratory. The proton beam current was
87 50 nA–1 μ A. Since the direct beam intensity was too strong for our purpose
88 even at a low current of 10 nA (10 year in-orbit equivalent protons would be
89 irradiated in less than one second), we used scattered protons. Use of scat-
90 tered protons provided another benefit that the large-CCD could be almost
91 uniformly damaged as is the actual case in space.

92 Figure 1 shows a top view of our experimental setup in a scattering cham-
93 ber of 1 m in diameter. The direct proton beam from the accelerator was

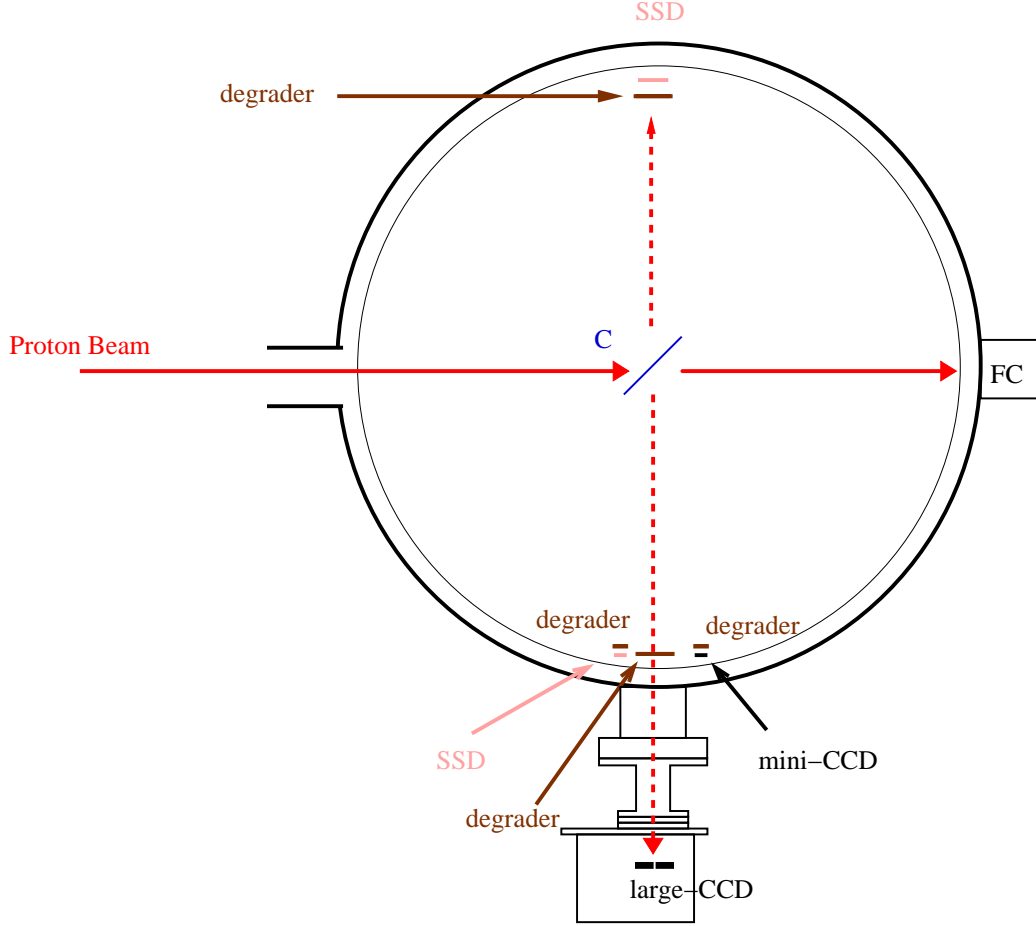


Figure 1: Top view of experimental setup in the scattering chamber of 1 m in diameter.

94 scattered at the center of the chamber. The large-CCD, which was installed
 95 in a camera body attached outside of the chamber via flange, was located at
 96 a right angle to the axis of the proton beam. The proton beam intensity was
 97 measured by a Faraday cup, and the energy spectra of the scattered protons
 98 were measured by silicon solid-state detectors.

99 A thin carbon foil of 15 mg cm^{-2} was used as a scattering target. The
 100 first excited energy level of ^{12}C nucleus is about 4.4 MeV that is large enough

101 to remove inelastic scattered protons using a thin aluminum degrader shown
 102 in Figure 1. The proton beam energy was 10.5 MeV, and protons incident
 103 on the CCDs through degraders were mono-energetic with a peak energy of
 104 6.7 MeV and a full width at half maximum of 0.9 MeV. The protons incident
 105 on the CCDs had a range of about 360 μm in silicon and easily penetrated
 106 our device with a thickness of 200 μm . Therefore, energy deposition was
 107 relatively uniform along the depth direction with 12–16 keV μm^{-1} . The
 108 total deposited energy in our device of single proton was about 2.7 MeV.

109 The large-CCD was operated in the camera body with a temperature
 110 of -110°C and the whole imaging area was irradiated with an ^{55}Fe source.
 111 The back bias voltage applied was 35 V. Degradation of the large-CCD was
 112 monitored alternating proton irradiation and ^{55}Fe data acquisition. On the
 113 other hand, the mini-CCD was placed without a camera system inside the
 114 chamber hence its gradual change was not monitored. Instead, the mini-CCD
 115 provided a higher dose data because of its closeness to the scattering target
 116 than the large-CCD. The ^{55}Fe data of the mini-CCD were taken before and
 117 after this experiment in our laboratory.

118 **3. Dose rate in the orbit of the Astro-H satellite and exposed dose** 119 **in this experiment**

120 In order to determine whether or not our device has radiation hardness
 121 enough for space use, it is necessary to estimate the dose rate in space and
 122 convert the exposed dose in this experiment to equivalent time in space. For
 123 the calculation of the dose rate, we referred to the day-averaged cosmic-ray
 124 flux model in the low earth orbit at an inclination angle of $\sim 30^{\circ}$ [17], in which

125 the Astro-H will fly. The cosmic-ray model shows that the geomagnetically-
 126 trapped proton in the South Atlantic Anomaly (SAA) is by far the largest
 127 population among high-energy particle and radiation components which can
 128 penetrate a surrounding camera body and reach the CCD inside. At least
 129 more than 90% of whole high-energy charged particles exposed to a satellite
 130 come from the SAA on a day-average basis (T. Mizuno, private communica-
 131 tion). We thus used the SAA proton component alone from the cosmic-ray
 132 model.

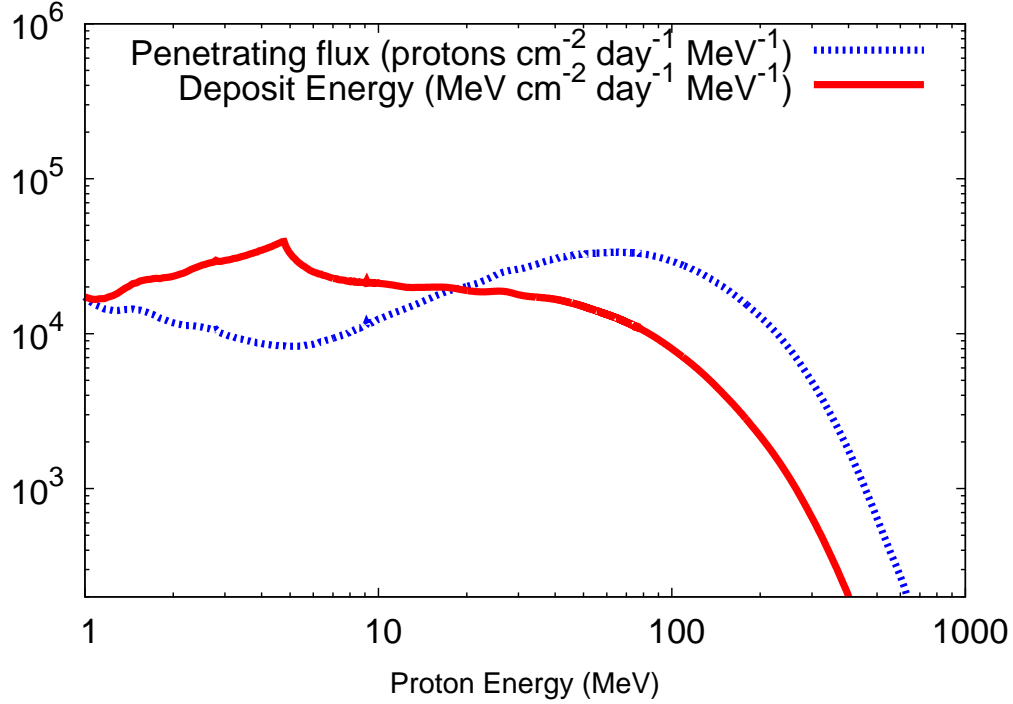


Figure 2: Number flux spectrum of protons that penetrate the camera body and reach the CCD (blue) and energy spectrum deposited from protons at the CCD (red).

133 Figure 2 shows a number flux spectrum of protons that penetrate the

134 camera body and reach the CCD. This spectrum was obtained from the
 135 SAA proton flux spectrum calculating their energy loss at the passage of
 136 the camera body. We approximated the camera body as an aluminum 2 cm
 137 thickness shell in this calculation. Figure 2 also shows an energy spectrum
 138 deposited from protons at the CCD. This spectrum was obtained multiplying
 139 the incoming proton number flux to the CCD with their energy deposition at
 140 the CCD that is a function of the proton energy. The incoming number flux
 141 spectrum has a peak around ~ 70 MeV, which is the threshold energy to pen-
 142 etrate 2 cm thick aluminum camera body. On the other hand, the deposited
 143 energy spectrum shows that lower energy proton population contributes more
 144 to the total dose at the CCD. Integrating the deposited energy spectrum, we
 145 obtained a dose rate of 2.2×10^6 MeV cm $^{-2}$ day $^{-1}$ or 260 rad year $^{-1}$. Un-
 146 certainty of this value was estimated to be at most a factor of 2 that mainly
 147 comes from the SAA proton flux spectrum (T. Mizuno, private communica-
 148 tion).

149 The total proton fluence exposed to the large-CCD and the mini-CCD
 150 were about 0.9 and 3.7×10^9 cm $^{-2}$, respectively. These values correspond to
 151 about 3 and 13 year in orbit, which covers the Astro-H satellite's mission life
 152 time of 5 years. The gradual degradation of the large-CCD was monitored
 153 at equivalent times in orbit of 2 days, 2 weeks, 2 months, 6 months, 1 year,
 154 2 years, and 3 years.

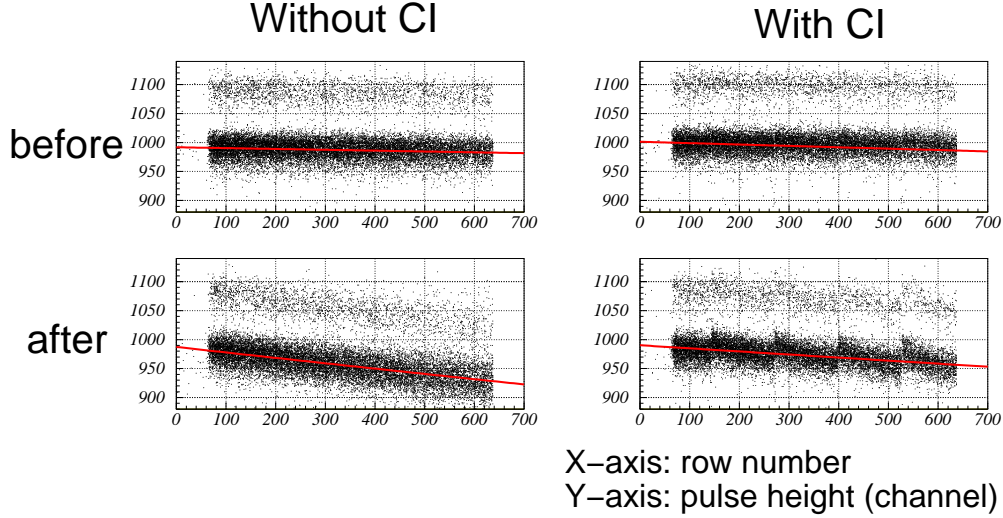


Figure 3: Stacking plots (black dots) with the best fit CTI function (red). Top and bottom figures show those before (no fluence) and after proton irradiation ($0.9 \times 10^9 \text{ cm}^{-2}$), while left and right figures show those without or with CI.

155 4. Result

156 4.1. Charge transfer inefficiency as a function of proton fluence

157 Figure 3 shows “stacking plots” made from ^{55}Fe irradiation data, in which
 158 pulse heights of the X-ray hit pixels are plotted as a function of row number
 159 that is namely half of the number of transfers in our case because of on-chip
 160 2×2 binning. Each stacking plot shows dense and faint bars which come
 161 from Mn $K\alpha$ and Mn $K\beta$ data, respectively. In the analysis, we used selected
 162 events in which the charge is in a single pixel, not be split into neighboring
 163 pixels.

164 Before the experiment (no fluence), the pulse height decline is barely seen
 165 along the row number. On the other hand, after the experiment (the proton
 166 fluence exposed was $0.9 \times 10^9 \text{ cm}^{-2}$), the pulse height clearly decreases as

167 a function of the row number due to an increase of the CTI. The scatter of
 168 the pulse height at a given row number also becomes larger, which is more
 169 evident in Mn $K\beta$ data in this figure. Comparing the bottom two plots, it is
 170 clear that applying the CI technique reduces radiation damage effects of this
 171 type: both the pulse height decline and scattering are mitigated. A “saw-
 172 tooth shape” seen in the bottom-right plot is the characteristic of applying
 173 the CI[14]. The degree of the mitigation is locally maximum just after the
 174 charge-injection row and decreases as apart from it. The regularly-spaced
 175 charge-injection rows thus make such a periodic pattern in the stacking plot.

The CTI value can be determined by fitting the stacking plots with the
 following function,

$$Q = Q_0 \times (1 - CTI)^{2Y}, \quad (1)$$

176 where Q_0 is the original charge produced by X-ray from ^{55}Fe , Q is the ob-
 177 served charge after transfer, and Y is the row number of the pixel hit by the
 178 X-ray. Red lines in Figure 3 show the best fit curves only using the Mn $K\alpha$
 179 data. The CTI value represents the slope of the stacking plot.

180 Figure 4 shows the CTI measured without applying the CI technique. The
 181 data are plotted as a function of proton fluence (top label) or equivalent time
 182 in orbit (bottom label). The colored circles indicate the data taken from our
 183 experiment. There are two segments (we call AB and CD) in the large-CCD
 184 as we used two readout nodes. Systematic uncertainties dominate and we
 185 estimated them as follows. We first divided the data into 10 subsets, derived
 186 the CTI value for each subset, and used a scatter of the values as a systematic
 187 uncertainty of the data, although they were still smaller than the radius of
 188 the circles in the figure. The black dots show the Suzaku BI CCD data

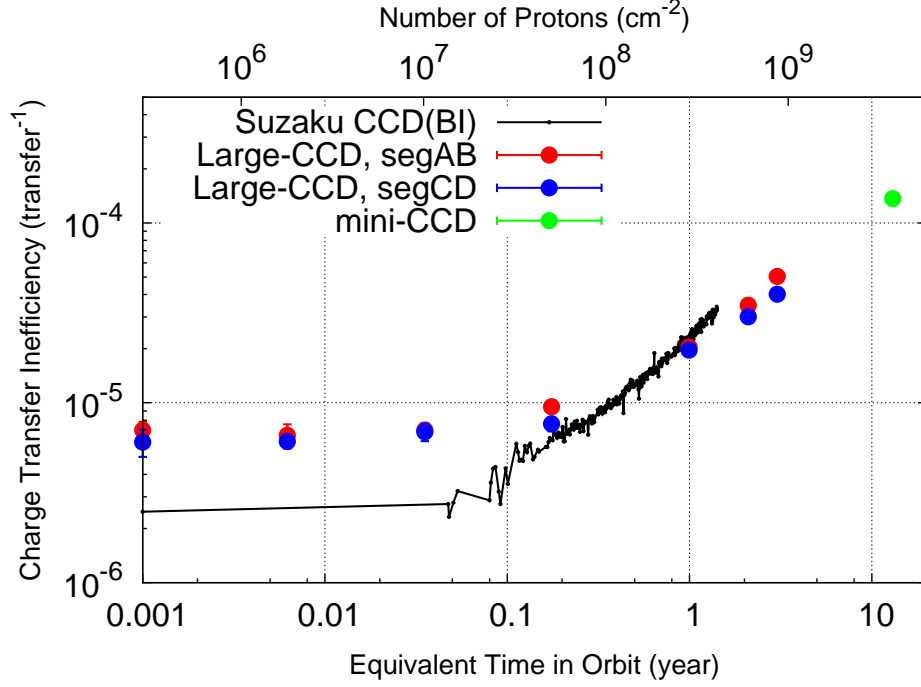


Figure 4: Charge transfer inefficiency measured without applying the CI technique. The data are plotted as a function of proton fluence (top label) or equivalent time in orbit (bottom label). Red and blue circles indicate the large-CCD data but from two different segments while green circles indicate the mini-CCD data. Black dots show Suzaku BI CCD data. Note that the data point equivalent to 6 month in orbit is lacking because of operation error.

189 actually taken in space. The Suzaku CCD has two ^{55}Fe calibration sources
 190 irradiating top corners of the imaging area (far side from readout nodes)[2].
 191 The calibration data was available on a daily basis and summarized on-line¹.
 192 We reproduced the CTI values based on the on-line data. Data points at
 193 0.001 year equivalent in orbit mean those before experiment or before launch.

¹see <http://space.mit.edu/XIS/monitor/ccdperf/>

194 In the case of our P-channel CCD, the CTI was measured to be 7.0×10^{-6}
 195 before experiment and more or less constant until about 1 month or so. It
 196 then went up to an order of 10^{-5} after 4.5 months, and reached to 5.0×10^{-5}
 197 at 3 year. The mini-CCD data point suggests that the CTI would rise with
 198 a similar slope up to about 13 year. This time evolution is similar to that of
 199 the Suzaku CCD data, especially in terms of the slope after a few months.
 200 The apparent difference between their slopes is likely due to the possible
 201 uncertainty of factor of 2 in the conversion of proton fluence to equivalent
 202 time in orbit.

203 Figure 5 shows the CTI measured with applying the CI technique. The
 204 definition of the marks and labels are the same as that of Figure 4. The
 205 mini-CCD data with the CI was not available. The Suzaku CCD had been
 206 operated without the CI until 1.2 year after the launch. After some verifi-
 207 cation tests[12], the CI was incorporated in the standard observation mode.
 208 Thus, the calibration data with the CI were also only available since about
 209 1 year after the launch. The amount of injected charge was increased from
 210 2 keV equivalent to 6 keV equivalent about 6 years after the launch, which
 211 reduced the CTI as shown in Figure 5.

212 Applying the CI technique reduces not only the CTI values themselves
 213 but also its growth rate: the reduction factors are 1.5, 1.8, and 2.0 in the last
 214 three data. This suggests that the CI works more efficiently when the device
 215 is more damaged at least in our case. The slope is again similar to that of
 216 the Suzaku CCD data. Our P-channel data appear to go along with the
 217 6 keV equivalent Suzaku CCD data rather than that of the 2 keV equivalent,
 218 although it may not be significant considering the uncertainty.

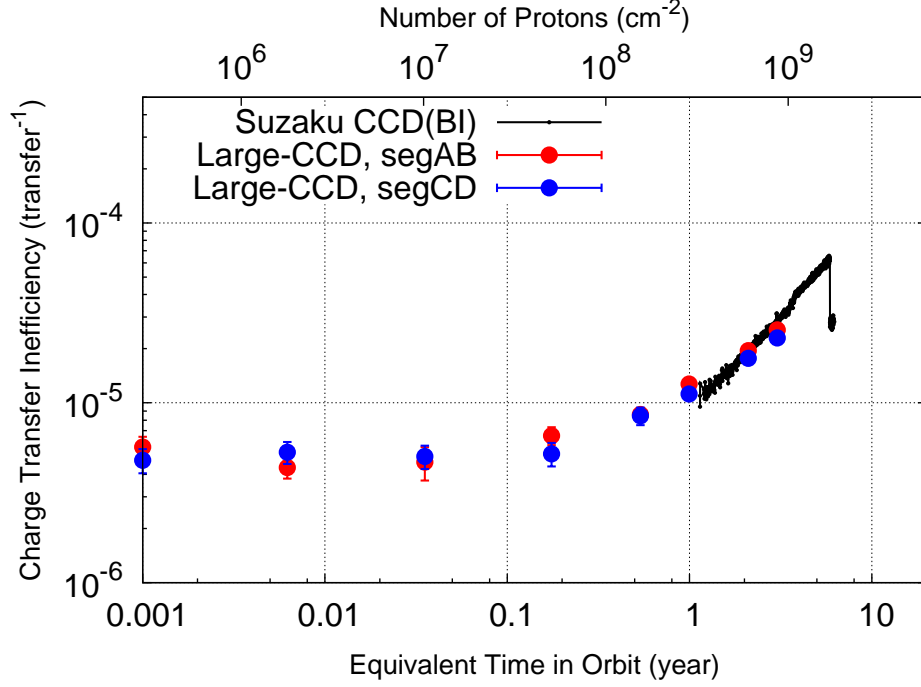


Figure 5: Charge transfer inefficiency measured with applying the CI technique. The data are plotted as a function of proton fluence (top label) or equivalent time in orbit (bottom label). Red and blue circles indicate the large-CCD data but from two different segments. Black dots show Suzaku BI CCD data. A discontinuous decrease of the CTI in the Suzaku data at 6 years after the launch is due to an increase of the amount of injected charge from 2 keV equivalent to 6 keV equivalent.

219 In the both cases with or without the CI, the degradation of the CCD
 220 performance in terms of the CTI is shown to be comparable with that of the
 221 Suzaku CCD. Applying the same ground-base CTI correction as those for
 222 the Suzaku CCD data to our P-channel CCD data, we can expect to provide
 223 the data with the similar quality as the Suzaku data.

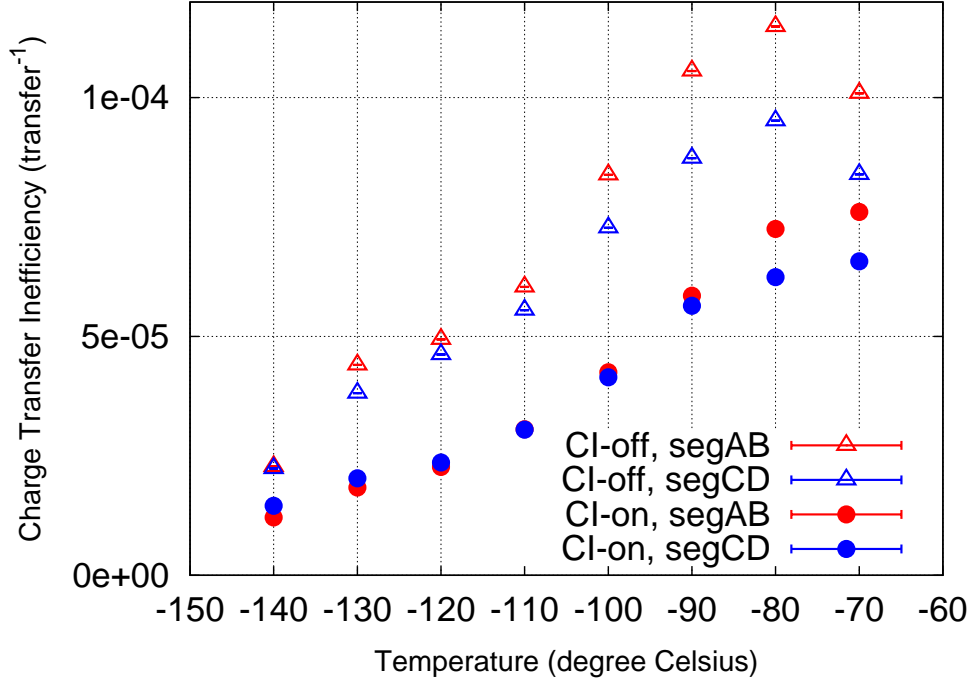


Figure 6: Charge transfer inefficiency measured as a function of the temperature of the CCD. Triangles and circles indicate the data without and with the CI, respectively. The different color indicate different segment data.

4.2. Charge transfer inefficiency as a function of temperature

Figure 6 shows the CTI measured as a function of the temperature of the CCD. These data were taken in our laboratory after the proton radiation damage experiment. The values are slightly different from those shown in previous figures even at the same temperature (-110 °C) probably because of partially used different electronics. Within the temperature range we tested, it is found that the CTI is smaller at lower temperature. The turn over of the data without the CI at -80°C is not real. At temperature higher than -90°C, a charge-trailing became obvious likely due to an increase of the number of

traps with a short detrapping time scale of a few CCD clock cycles[2]. In such a situation, using a single pixel data introduces a selective bias and the CTI would be falsely evaluated to be smaller. The difference between the two segments is also smaller at the lower temperature. The effect of applying the CI technique reducing the CTI by about a factor of 2 is almost the same regardless of the temperature.

5. Discussion

We performed a proton radiation damage experiment on our newly developed P-channel CCD and confirmed that its radiation hardness is comparable with that of the Suzaku N-channel CCD actually working in space. Although this result verifies the validity of space use of our P-channel CCD, it might contradict with the previous report that P-channel CCDs are radiation harder than N-channel CCDs.

Figure 7 shows a comparison between our results and those reported from another team using a P-channel CCD made by the Lawrence Berkeley National Laboratory (LBNL) [8]. There were two types of the LBNL CCDs whose data were published: one had the “notch” structure and the other did not. The notch structure, a narrow implant in the CCD channel confining a charge packet to a fraction of the pixel volume in an additional potential well, has been known to reduce the CTI[18, 8]. In order to make a direct comparison, we plot our P-channel CCD data without applying the CI and the LBNL P-channel CCD data without the notch structure. A simple comparison along the number of protons irradiated indicates that the LBNL CCD may have about an order of magnitude higher radiation tolerance compared

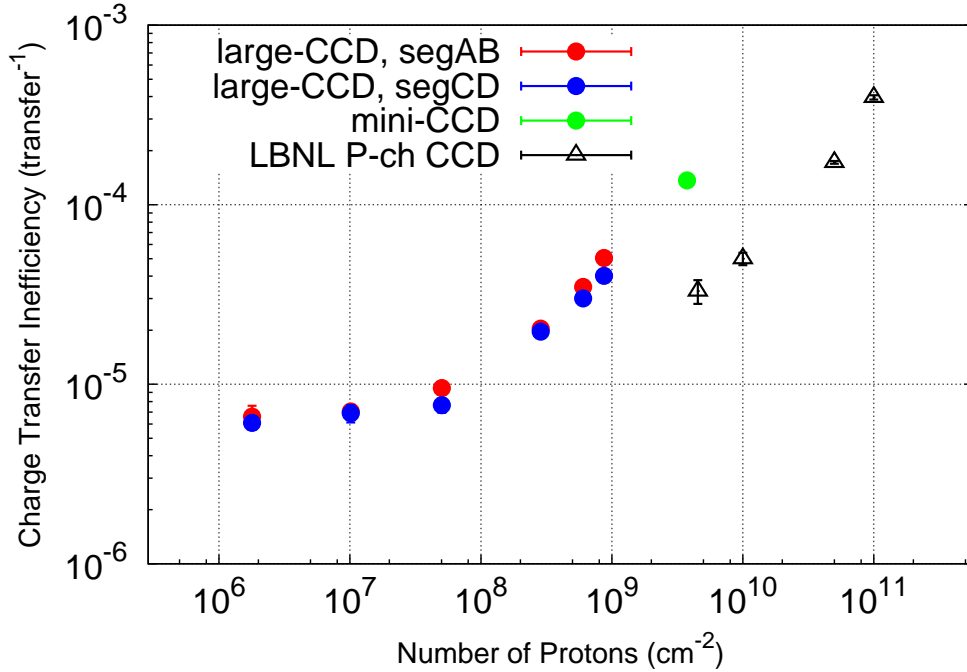


Figure 7: A comparison of the radiation hardness of our P-channel CCD without applying the CI (colored circles) and the LBNL P-channel CCD without the notch structure (black triangles). The data of the LBNL P-channel CCD are taken from Bebek et al. (2002)[8].

257 to our CCD. This difference can not be resolved even considering the differ-
 258 ences in the incident proton energies and the CCD temperatures between the
 259 two experiments. In the LBNL CCD experiment, the incident proton energy
 260 and the CCD temperature were 12 MeV and -145°C, respectively. The en-
 261 ergy deposit of the 12 MeV protons is about a factor of 2 lower than that of
 262 6.7 MeV protons used in our experiment. From figure 6, lowering the CCD
 263 temperature from -110°C to -145°C would reduce the CTI by about a factor
 264 of 2. Thus, about a factor of 4 difference can be explained by the difference
 265 in the experimental setup. However, significant difference in the radiation

266 hardness still remains between the two P-channel CCDs. The different man-
267 ufacturing process might be a reason but we do not have a clear answer at
268 this moment.

269 The LBNL CCD experiment was performed while the devices were un-
270 powered and at room temperature. On the other hand, the large-CCD was
271 powered and cooled during our proton irradiation experiment. However, this
272 difference does not appear to affect the degree of the damage at least in
273 terms of the CTI, considering the relatively smooth connection between the
274 large-CCD and the mini-CCD data. The same conclusion was deduced for
275 N-channel CCDs in a similar proton radiation experiment[19].

276 The temperature dependency measurement described in section 4.2 was
277 performed in our laboratory about two months after the proton radiation
278 damage experiment. Meanwhile the large-CCD was kept at room tempera-
279 ture. A CTI measurement at the same CCD temperature showed about a
280 40% worse value compared to the last value obtained at the accelerator lab-
281 oratory. As we previously noted, this apparent degradation was most likely
282 due to a partial difference of electronics used. This fact then suggests that an
283 annealing at room temperature did not help to restore the radiation damage
284 for our device at least at this damage level.

285 We confirmed that applying the CI technique and lowering the CCD
286 temperate are both efficient methods to mitigate the radiation damage. Al-
287 though we tentatively spaced the CI rows 128 row apart in this experiment,
288 the Suzaku CCD camera injects charges at every 54 row. We can expect
289 further reduction of the CTI by narrowing the spacing of the CI rows. Since
290 too many CI rows also reduce an effective imaging area, we need to find out

291 an optimized spacing in future experiments.

292 The temperature dependence of the CTI of the damaged CCDs varies
293 device to device[15, 16]. Therefore, the understating of the temperature
294 dependence allows us a flexible operation in space where the power available
295 is quite limited. For example, it is a possible option for us to operate the
296 CCD with -100°C in the initial phase and -120°C in the later phase of the
297 mission based on this result.

298 **Acknowledgment**

299 We would like to thank all the SXI team members. We also appreciate
300 Dr. T. Mizuno who kindly provided the cosmic-ray flux model used in this
301 report, Dr. M. Kokubun for useful comments, and the Suzaku XIS team at
302 MIT for making the ^{55}Fe monitoring data available on-line. This work was
303 supported by JSPS KAKENHI Grand Number 23000004.

304 **References**

- 305 [1] Y. Tanaka, H. Inoue, S. S. Holt, The X-ray astronomy satellite ASCA,
306 PASJ 46 (1994) L37–L41.
- 307 [2] K. Koyama, et al., X-Ray Imaging Spectrometer (XIS) on Board Suzaku,
308 PASJ 59 (2007) 23–33.
- 309 [3] D. Matsuura, et al., Development of p-Channel Charge-Coupled De-
310 vice for NeXT, the Next Japanese X-ray Astronomical Satellite Mission,
311 Japanese Journal of Applied Physics 45 (2006) 8904.

- 312 [4] H. Tsunemi, et al., Soft x-ray imager (SXI) onboard ASTRO-H, in:
313 Society of Photo-Optical Instrumentation Engineers (SPIE) Conference
314 Series, volume 7732 of *Society of Photo-Optical Instrumentation Engineers (SPIE) Conference Series*.
315
- 316 [5] K. Hayashida, et al., Development of the soft x-ray imager (SXI) for
317 ASTRO-H, in: Society of Photo-Optical Instrumentation Engineers
318 (SPIE) Conference Series, volume 8145 of *Society of Photo-Optical Instrumentation Engineers (SPIE) Conference Series*.
319
- 320 [6] T. Takahashi, et al., The ASTRO-H Mission, in: Society of Photo-
321 Optical Instrumentation Engineers (SPIE) Conference Series, volume
322 7732 of *Society of Photo-Optical Instrumentation Engineers (SPIE) Conference Series*.
323
- 324 [7] G. R. Hopkinson, Proton damage effects on p-channel CCDs, IEEE
325 Transactions on Nuclear Science 46 (1999) 1790–1796.
- 326 [8] C. Bebek, D. Groom, S. Holland, A. Karcher, W. Kolbe, J. Lee, M. Levi,
327 N. Palaio, B. Turko, M. Uslenghi, A. Wagner, G. Wang, Proton radiation
328 damage in p-channel CCDs fabricated on high-resistivity silicon, IEEE
329 Transactions on Nuclear Science 49 (2002) 1221–1225.
- 330 [9] C. J. Marshall, P. W. Marshall, A. Wacynski, E. Polidan, S. D. Johnson,
331 A. Campbell, Comparisons of the proton-induced dark current and
332 charge transfer efficiency responses of n- and p-channel CCDs, in: J. D.
333 Garnett, J. W. Beletic (Eds.), Society of Photo-Optical Instrumentation
334 Engineers (SPIE) Conference Series, volume 5499 of *Society of Photo-*

- 335 *Optical Instrumentation Engineers (SPIE) Conference Series*, pp. 542–
336 552.
- 337 [10] J. P. Spratt, The effects of nuclear radiation on P-channel CCD imagers,
338 IEEE Radiation Effects Data Workshop (1997) 116–121.
- 339 [11] M. Bruzzi, Radiation damage in silicon detectors for high-energy physics
340 experiments, IEEE Transactions on Nuclear Science 48 (2001) 960–971.
- 341 [12] M. W. Bautz, et al., Mitigating CCD radiation damage with charge
342 injection: first flight results from Suzaku, in: Society of Photo-Optical
343 Instrumentation Engineers (SPIE) Conference Series, volume 6686 of
344 *Society of Photo-Optical Instrumentation Engineers (SPIE) Conference*
345 *Series*.
- 346 [13] H. Nakajima, et al., Performance of the Charge-Injection Capability of
347 Suzaku XIS, PASJ 60 (2008) 1.
- 348 [14] H. Uchiyama, et al., New CTI Correction Method for Spaced-Row
349 Charge Injection of the Suzaku X-Ray Imaging Spectrometer, PASJ
350 61 (2009) 9.
- 351 [15] S. Sembay, A. Abbey, B. Altieri, R. Ambrosi, D. Baskill, P. Fer-
352 rando, K. Mukerjee, A. M. Read, M. J. L. Turner, In-orbit perfor-
353 mance of the EPIC-MOS detectors on XMM-Newton, in: G. Hasinger,
354 M. J. L. Turner (Eds.), Society of Photo-Optical Instrumentation Engi-
355 neers (SPIE) Conference Series, volume 5488 of *Society of Photo-Optical*
356 *Instrumentation Engineers (SPIE) Conference Series*, pp. 264–271.

- 357 [16] C. E. Grant, M. W. Bautz, S. E. Kissel, B. LaMarr, G. Y. Prigozhin,
358 Temperature dependence of charge transfer inefficiency in Chandra x-ray
359 CCDs, in: Society of Photo-Optical Instrumentation Engineers (SPIE)
360 Conference Series, volume 6276 of *Society of Photo-Optical Instrumen-*
361 *tation Engineers (SPIE) Conference Series*.
- 362 [17] T. Mizuno, et al., Monte Carlo simulation study of in-orbit background
363 for the soft gamma-ray detector on-board ASTRO-H, in: Society of
364 Photo-Optical Instrumentation Engineers (SPIE) Conference Series, vol-
365 ume 7732 of *Society of Photo-Optical Instrumentation Engineers (SPIE)*
366 *Conference Series*.
- 367 [18] H. Tsunemi, M. Miki, E. Miyata, Application of a mesh experiment for
368 a proton beam onto the charge-coupled device, IEEE Transactions on
369 Nuclear Science 51 (2004) 2288–2292.
- 370 [19] E. Miyata, T. Kamazuka, H. Kouno, M. Fukuda, M. Mihara, K. Mat-
371 suta, H. Tsunemi, K. Tanaka, T. Minamisono, H. Tomida, K. Miyaguchi,
372 Proton Irradiation Experiment for X-ray Charge-Coupled Devices of
373 the Monitor of All-Sky X-ray Image Mission Onboard the International
374 Space Station: I. Experimental Setup and Measurement of the Charge
375 Transfer Inefficiency, Japanese Journal of Applied Physics 41 (2002)
376 7542.